ELSEVIER

Journal of Marine Systems 18 (1998) 161–178

JOURNAL OF MARINE SYSTEMS

A wind-driven circulation model of the Tyrrhenian Sea area

S. Pierini *, A. Simioli

Istituto di Meteorologia e Oceanografia, Istituto Universitario Navale, Corso Umberto I, 174-80138 Napoli, Italy

Received 1 December 1996; accepted 16 June 1997

Abstract

The wind-driven component of the circulation in the Tyrrhenian Sea area was analyzed by means of a free-surface, barotropic primitive equation model implemented in the whole Mediterranean Sea. The 'National Meteorological Center' (NMC) wind data covering the period 1980–1988 were used to force the model. Both the seasonal and the high frequency variability were studied. For the first case, a perpetual wind forcing was constructed by instantaneously averaging the wind stresses over the 9 years, and the response was Fourier filtered in order to get rid of the residual rapid fluctuations. The daily variability was then produced for the test years 1981 and 1987 by making use of the instantaneous forcing. The main features of the wind-driven climatological Tyrrhenian circulation known from data and general circulation modelling were found to be reproduced by this process model. The winter cyclonic circulation induced by the strong positive wind vorticity input evolved into a much weaker, partially reversed circulation in summer months. A mainly northward flux through the strait of Corsica and a horizontally sheared current in the strait of Sicily were found. The rapid fluctuations that the wind was able to induce in the ocean were then studied. The instantaneous currents were found to be up to 10 times larger than the corresponding climatological ones, with episodes of reversal over a period of few days. The experimental evidence of the existence of these rapid wind-driven fluctuations is discussed. The analysis of the daily variability provides a realistic picture of the character of the wind-driven circulation in the Tyrrhenian Sea that differs considerably from the classical seasonal dynamics. As an indicator of the Tyrrhenian Sea dynamics, the mass transport through the strait of Corsica was evaluated for the year 1987 and compared with available experimental data. As a result, the low-passed wind-driven transport reflects the seasonal trend and accounts for 15–40% of the total (the remaining part being induced by thermal effects and the remote Gibraltar forcing). Moreover, the high frequency variability modulates the seasonal signal, with a comparable r.m.s. Finally, the interaction between the wind-driven dynamics in the straits of Corsica, Sicily and Sardinia and that in the interior of the Tyrrhenian Sea was studied by means of an ad hoc numerical experiment. As a result, a one-way interaction was found. The Tyrrhenian wind-driven dynamics appears to be mainly forced by the local winds, while the fluxes through the straits are mainly driven by the internal circulation.

Keywords: Tyrrhenian Sea; Wind-driven circulation model; Barotropic primitive equation model; Wind stress; Fourier filter

1. Introduction

It is a relatively new but well established result that the circulation in the Mediterranean Sea presents important seasonal variations that can be locally more intense than the annual mean. The deviations

* Corresponding author. Present address: Dipartimento di Fisica, Universitá dell' Aquila, 67010 Coppito (C'Aquila), Italy.

0924-7963/98/$ - see front matter
PII: S0924-7963(98)00010-4

from the seasonal climatology from year to year can also be very large. This seasonal and interannual variability was assessed by recent observations (e.g., Béthoux, 1980; Millot, 1987; Robinson et al., 1991; Tziperman and Malanotte-Rizzoli, 1991; Astraldi et al., 1990) and numerical modelling (Heburn, 1987, 1994; Malanotte-Rizzoli and Bergamasco, 1989, 1991; Stanev et al., 1989; Beckers, 1991; Pinardi and Navarra, 1993; Herbaut et al., 1996, 1997; Roussenov et al., 1995; Zavatarelli and Mellor, 1995; Korres et al., 1995a,b; Pinardi et al., 1996). The main driving mechanisms that come into play are the heat, evaporative and momentum fluxes at the air–sea interface, the fluxes of Atlantic water (AW) and modified Levantine intermediate water (MLIW) through the Strait of Gibraltar and the fresh water river discharges. The barotropic component of the circulation is mainly wind-driven and is highly dependent on the topography of the basin. It is composed of subbasin scale gyres that can be more or less seasonally variable and recurrent. The thermohaline circulation is forced by heat and evaporative fluxes and is shaped by mechanisms of water mass formation and deep convection. The baroclinic dynamics is also affected by internal dynamical processes which typically give rise to a mesoscale eddy field.

Among all the Mediterranean subbasins the Tyrrhenian Sea is, to some extent, peculiar in that its dynamics shows a very pronounced barotropic component. An almost basin-wide cyclonic circulation at all depths is present during winter, accompanied by a highly barotropic northward flow through the Corsica channel and by a northeastward flow of LIW through the Sicily channel joined by a flow of modified AW coming from the Sardinia channel, which then follows the same cyclonic motion; in late spring and in summer, a remarkable weakening and a local reversal of the flow is observed (e.g., Krivosheya and Ovchinnikov, 1973; Millot, 1987; Astraldi and Gasparini, 1992, 1994; Astraldi et al., 1994).

The importance of the barotropic component in the Tyrrhenian circulation suggests that the wind is likely to play a major role as a forcing agent. This is, for instance, supported by the fact that a purely wind-driven model of the Mediterranean (Pinardi and Navarra, 1993) provides a seasonal signal in this subbasin that is similar to that obtained in the framework of general circulation models in which the thermal and evaporative forcings are fully taken into account (Roussenov et al., 1995; Zavatarelli and Mellor, 1995). On the other hand, the fluxes of AW and LIW through the strait of Gibraltar give an important contribution to the dynamics of the western Mediterranean and also the Tyrrhenian Sea dynamics is affected by such remote forcing, as proved by Herbaut et al. (1996). These constitute examples of process studies in which only one driving mechanism is considered: to the extent that different forcings produce effects that are weakly interacting, such simplified modelling studies are able to give some answer to the question of what are the main causes of a given circulation structure, and how these causes act compared with other sources of energy.

In this context, we present a wind-driven circulation model of the whole Mediterranean Sea based on the shallow-water equations driven by the 'National Meteorological Center' (NMC) winds with the aim of analyzing—with a process study approach—different aspects of the wind-driven dynamics of the Tyrrhenian Sea. After a discussion of the model and the forcing used (Section 2) the seasonal variability is obtained by forcing the system through a perpetual wind forcing and the analysis is carried out after having Fourier filtered the response (Section 3). The main features of the barotropic Tyrrhenian circulation known from data and general circulation modelling are found to be reproduced by this process model.

In Section 4 we consider the high frequency—daily—variability of the flow. This aspect of the circulation is usually neglected in general circulation models since, certainly, the seasonal and interannual variabilities are the most distinctive features of each oceanic basin and therefore deserve primary attention. However, understanding the basic mechanisms that produce the rapid barotropic response to winds in an oceanic region is relevant for short term ocean forecasting, a branch of applied physical oceanography that is receiving increasing attention. Moreover, the effect that retaining the high frequency variability has in the dispersion properties of the flow is still to be fully understood, but there are general results indicating that it actually may be important to this respect (e.g., Pierrehumbert, 1990; Pierini and Zambianchi, 1997). In the study of Section 4, the daily

signal is produced by forcing the system with instantaneous NMC data, and is found to be usually larger than the seasonal one, with pronounced spatial variabilities over periods of even 1—2 days. The experimental evidence that such variability is indeed present in the Tyrrhenian Sea is finally discussed.

In Section 5, we then compare the 1987 wind-driven transport through the strait of Corsica produced by the model and the total transport measured in the same strait, in consideration of its character of good indicator of the global Tyrrhenian circulation. Such comparison allows to conclude that the 1987 wind-driven seasonal transport appears to have accounted for about 15–40% of the total (depending on the choice of the horizontal eddy viscosity coefficient) while the high frequency wind-driven part of the transport had a r.m.s. comparable to that of the total seasonal signal.

Finally, in Section 5, we also analyze the interaction between the wind-driven dynamics in the straits of Corsica, Sicily and Sardinia and in the interior of the Tyrrhenian Sea. This is to assess the importance of the channel fluxes in establishing the internal circulation. The comparison between the dynamics produced by the model of the whole Mediterranean and that derived by considering a 'closed' Tyrrhenian puts in evidence the very little influence that the channel fluxes have on the Tyrrhenian circulation. On the other hand, the latter, which thus appears to be locally wind-driven, controls the channel fluxes either by blocking or entraining them following the main circulation patterns.

2. The model equations and the 'NMC' forcing

The first direct effect produced in the ocean by the wind stress at the air–sea interface is the transfer of energy and momentum in the form of surface Ekman currents. Furthermore, because of the Ekman pumping mechanism and of the presence of coasts, a surface topography is produced and—consequently—pressure-driven geostrophic currents are generated. The latter are barotropic and often more energetic, so one can say that the main effect of the wind is the generation of an essentially barotropic circulation. In a purely wind-driven process-oriented study, one can then make use of equations specifically derived for the depth-averaged horizontal velocities, i.e., for the so-called barotropic component of the motion. In a hydrostatic context, the vertical integration of the two horizontal momentum equations and the imposition of the continuity of the stress at the bottom and at the sea surface leads to:

$$\boldsymbol{u}_t + (\boldsymbol{u}\cdot\nabla)\boldsymbol{u} + \boldsymbol{N}[\boldsymbol{u},\boldsymbol{u}'] + f\boldsymbol{k}\times\boldsymbol{u} = -\frac{1}{\rho_o}\nabla p + \frac{(\tau_w - \tau_b)}{\rho_o H} + A_H\nabla^2\boldsymbol{u} - \frac{g}{\rho_o H}\int_{-H}^{O} dz \int_z^O \nabla\rho\, dz' \qquad (1)$$

where $\boldsymbol{u}(\boldsymbol{x},t) = \frac{1}{H}\int_{-H}^{O}\boldsymbol{U}(x,z,t)dz$ is the depth-averaged horizontal velocity ($\boldsymbol{u} = (u,v)$, $\boldsymbol{x} = (x,y)$, $\boldsymbol{U}$ is the current velocity), p is the surface pressure, ρ is the density, ρ_o is a reference density, $f = f_o + \beta y$ is the Coriolis parameter, $\boldsymbol{k} = (0,0,1)$, g is the acceleration of gravity, A_H the horizontal eddy viscosity coefficient, τ_w is the wind stress, τ_b is the bottom stress and $H = D + \eta - d$ (where D is the mean water depth, $d(\boldsymbol{x})$ the bottom topography and $\eta(\boldsymbol{x},t)$ the free surface displacement). $\boldsymbol{N}$ includes the nonlinear interactions between the *barotropic* velocity $\boldsymbol{u}$ and the *baroclinic* velocity $\boldsymbol{u}' = \boldsymbol{U} - \boldsymbol{u}$.

Eq. (1) can be simplified by neglecting the baroclinic forcing term (the last term on the r.h.s.) representing the so-called Jebar effect (e.g., Holland, 1973; Huthnance, 1984). This was found to be small in the Mediterranean by Pinardi and Navarra (1993), who obtained a comparable response if in their wind-driven general circulation model the stratified ocean is substituted by a homogeneous fluid. Also the nonlinear terms $\boldsymbol{N}$ are found to be negligible by the same authors. It should be noticed that the omission of the baroclinic and nonlinear interactive terms simplifies considerably the model equations because in this case the barotropic dynamics is completely decoupled from the baroclinic one, and the ocean can be assumed as homogeneous. In conclusion, the baroclinic-free version of Eq. (1) with $\boldsymbol{N}$ set to zero, together with the classical vertically integrated continuity equation (e.g., Pedlosky, 1987) give the well known shallow-water equations

$$\begin{cases} \boldsymbol{u}_t + (\boldsymbol{u}\cdot\nabla)\boldsymbol{u} + f\boldsymbol{k}\times\boldsymbol{u} = -g\nabla\eta + \dfrac{(\tau_w - \tau_b)}{\rho_o H} + A_H\nabla^2\boldsymbol{u} \\ \eta_t + \nabla(H\boldsymbol{u}) = O \end{cases} \qquad (2)$$

where the surface pressure is converted in terms of the free surface elevation (we again stress that $\boldsymbol{u}$ is

the vertically averaged velocity, including the Ekman transport and the pressure-driven velocity). Unlike some of the general circulation models quoted above that have a rigid-lid as the upper vertical boundary, the present model has a dynamically active free surface. This turns out to be of fundamental importance in the analysis of the response to the high frequency winds (Section 4).

The initial-value problem for Eq. (2) with vanishing initial conditions and free-slip boundary conditions is solved by means of an explicit leap-frog finite difference scheme on the Arakawa C-grid (Pierini, 1996). The domain of integration (the Mediterranean sea with a closed Strait of Gibraltar and without the northern Adriatic sea) and the bottom topography used are shown in Fig. 1. The horizontal resolution is $\Delta x = \Delta y = 25$ km which corresponds approximately to $1/4°$, the temporal resolution is $\Delta t = 16$ s, $f_o = 0.89 \times 10^{-4}$ rad/s and $\beta = 1.825 \times 10^{-11}$ rad/(m · s), corresponding to a β-plane centered at 37.5° (we noticed that despite the small meridional extension, the βy correction to f_o is not completely negligible since we found that the flow can locally depart from the corresponding one on the f-plane by a small percentage). The eddy viscosity is chosen as $A_H = 5000$ m^2/s (see Section 5 for a discussion about this choice) and a quadratic bottom stress $\tau_b = \rho C_{Db} |\boldsymbol{u}| \boldsymbol{u}$ is used, with $C_{Db} = 0.002$. Note that the nonlinear terms in Eq. (2) are always found to be virtually negligible.

Let us pass to describe the NMC wind forcing. The original NMC (Washington, DC) 1000 mb data contain the following meteorological parameters: air velocity, air temperature and relative humidity (the whole data set was used in GCMs of the Mediterranean by Roussenov et al. (1995) and Pinardi et al. (1996)). The resolution is $1° \times 1°$ in space and 12 h in time. We computed the wind stress $\tau_w = \rho_a C_D |\boldsymbol{W}| \boldsymbol{W}$ (where ρ_a is the air density and $\boldsymbol{W}$ is the wind velocity) by using the drag coefficient according to Smith (1980).

$$\begin{cases} C_D = 10^{-3} & |\boldsymbol{W}| \le 6 \text{ m/s} \\ C_D = (0.61 + 0.063 \cdot |\boldsymbol{W}|) \cdot 10^{-3} & 6 \text{ m/s} < |\boldsymbol{W}| \le 22 \text{ m/s} \\ C_D = 2 \cdot 10^{-3} & 22 \text{ m/s} |\boldsymbol{W}| \end{cases}$$

In the study of the daily variability (Section 4) the instantaneous wind stress is considered. On the other hand, in order to study the seasonal variability (Section 3) a climatological, *perpetual* wind stress is computed by averaging the wind stress vectors over the 9 available years at any sampling time. We believe that averaging the stresses is more appropriate than averaging the winds and then compute the stresses as done by Roussenov et al. (1995), because if an average response over the 9 years is to be looked for, then—under the assumption of the linearity of the wind-driven problem—this can be obtained from a single run by using a forcing (the surface stresses) averaged over all the available years.

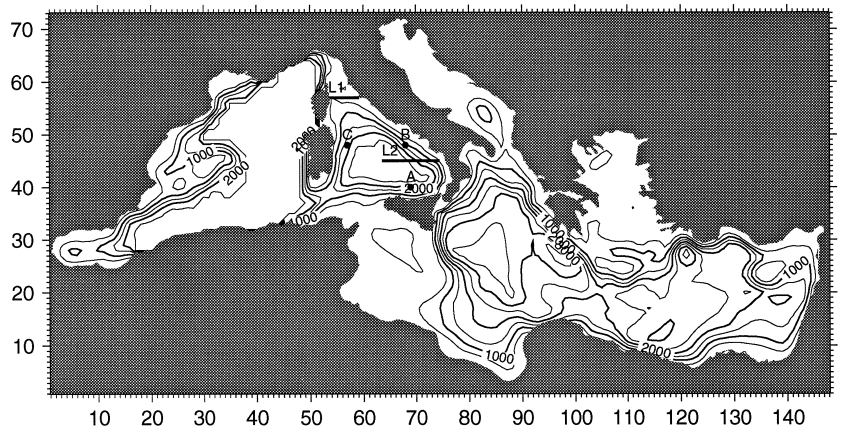

Fig. 1. The domain used in the numerical integration and the sea depth in meters. The coordinates are in multiples of the grid step $\Delta x = \Delta y = 25$ km.

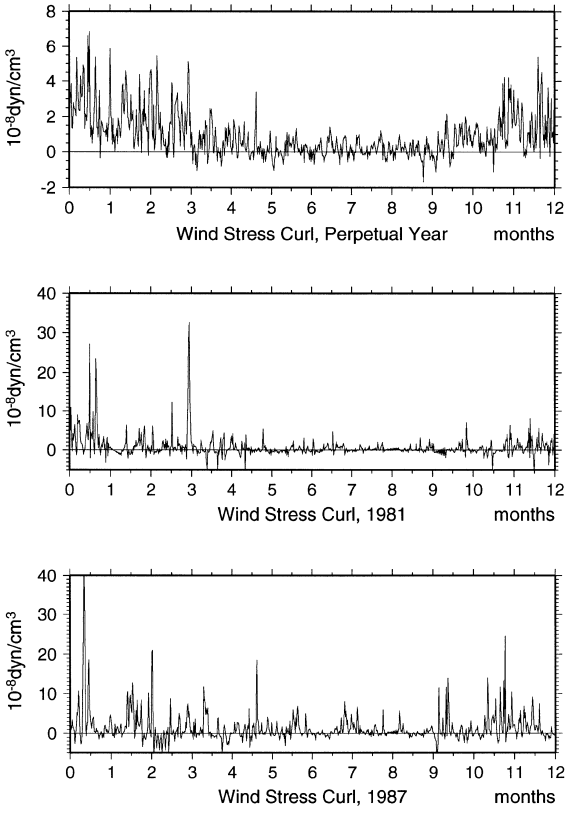

Fig. 2. Wind stress curl in a point in the middle of the Tyrrhenian Sea for the perpetual year and for the test years 1981 and 1987.

Finally, a wind stress field suitable for the model is constructed by performing a bilinear interpolation over the regular model grid at each sampling time, and then by linearly interpolating the winds at intermediate times (Pierini, 1996).

In Fig. 2, the wind stress curl in a point located in the middle of the Tyrrhenian Sea is shown for the perpetual year and for the test years 1981/1987. One can notice the different character of the perpetual year with respect to the 2 'instantaneous' years. The climatological averaging eliminates large peaks and reduces notably the total variance and the high frequency energy content. The resulting time series still retains much energy at high frequencies and has positive values except during the period June–September, when it attains small negative values. The response to the perpetual year forcing will be analyzed in Section 3, while the currents induced by the 1981/1987 winds will be considered in Section 4.

3. The seasonal variability

Let us start by analyzing the basin-scale winter and summer characteristics of winds and currents by considering the January and June monthly averages of the perpetual year winds and response (Figs. 3 and 4). Thanks to the basic linearity of the problem this is virtually equivalent to considering the monthly means for the wind forcing, as usually done in general circulation models of the Mediterranean (the circulation is represented by the sea surface elevation, which over this time scales is essentially proportional to the barotropic stream-function). An al-

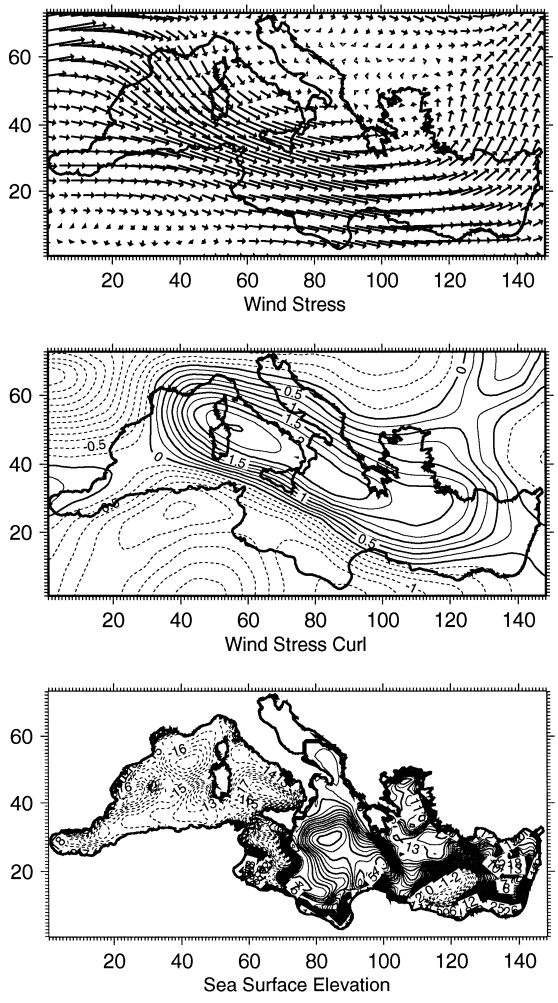

Fig. 3. January monthly averages of the perpetual wind stress, wind stress curl and induced sea surface elevation.

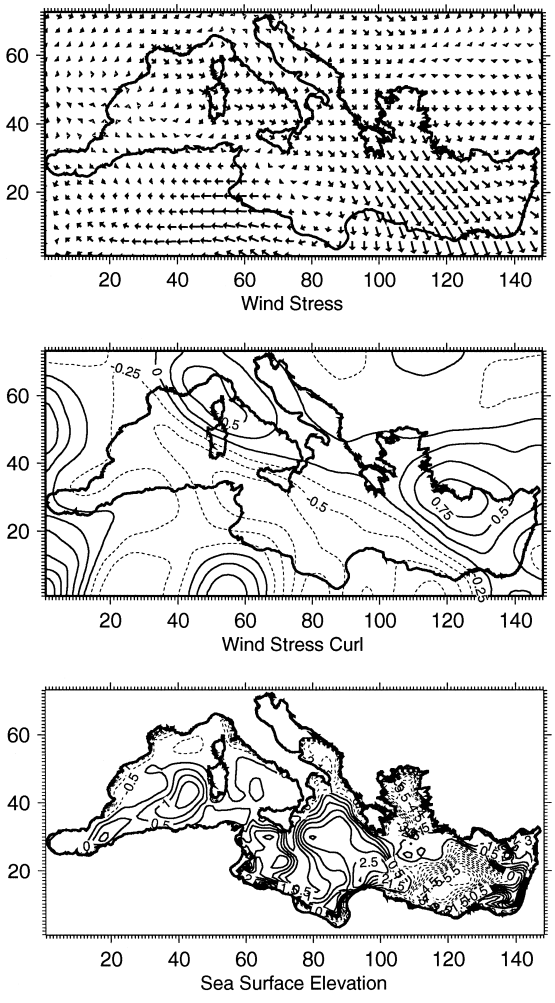

Fig. 4. June monthly averages of the perpetual wind stress, wind stress curl and induced sea surface elevation.

most basin-wide cyclonic circulation is present during winter, being induced by the intense positive vorticity input due to the wind, which is composed of a strong Mistral jet located in the southern part of the basin. Also the northern part of the Liguro–Provençal basin shows a similar wind-driven cyclonic circulation (note the position of the zero curl isoline in Fig. 3). In early summer the Mistral is greatly reduced and its location is shifted northward (Fig. 4). This in turn induces an appreciably lower circulation regime in the Tyrrhenian, which is also associated to an almost basin-wide reversal of the currents. These gross features of the wind-driven barotropic Tyrrhenian circulation are in agreement with the experimental (e.g., Krivosheya and Ovchinnikov, 1973; Millot, 1987; Hopkins, 1988; Astraldi and Gasparini, 1994) and theoretical (Pinardi and Navarra, 1993; Beckers et al., 1994; Heburn, 1994; Herbaut et al., 1996, 1997; Roussenov et al., 1995; Zavatarelli and Mellor, 1995) knowledge of the Tyrrhenian Sea dynamics.

In order to have a more complete information on the temporal evolution of the circulation, the classical monthly mean response should be replaced by the instantaneous response to winds. To this respect, stick-diagrams are shown (Fig. 5a) referring to three points inside the Tyrrhenian basin (see Fig. 1). This way of representing the seasonal circulation complements in a valuable way the traditional representation in terms of few snapshots of the circulation patterns. Moreover, in order to get rid of the residual high frequency energy left after the climatological averaging, the currents are filtered by retaining only six components in the Fourier series representation of the perpetual year response:

$$\boldsymbol{u}_{i,j}(t) \cong \tilde{\boldsymbol{u}}_{i,j}^{(o)} + \sum_{n=1}^{6} \tilde{\boldsymbol{u}}_{i,j}^{(n)} \cos\left(n\omega t + \varphi_{i,j}^{(n)}\right) \qquad (3)$$

where (i,j) identifies the grid point, $\omega = 2\pi/(1$ year) and $\tilde{\boldsymbol{u}}_{i,j}^{(n)}$ and $\varphi_{i,j}^{(n)}$ are the Fourier amplitudes and phases (an analogous harmonic analysis, but limited to the perpetual winds, was performed by Pinardi and Navarra (1993)). Fig. 5b shows that a cyclonic circulation (northwestward currents in point B and southwestward currents in point C) is present —on average—from the beginning of October until the end of May, with maximum currents in January–February. From June through September reversed currents are present, but with substantially lower amplitudes. The currents north of Sicily (point A) follow the same variation, belonging to the southern branch of the same circulation pattern. The amplitudes, of only few millimeter/second, are not expected to represent real values because of the reduced variance of the perpetual forcing, as discussed at the end of Section 2 (for more realistic values, see Section 4).

A synoptic view of the typical winter and summer circulation patterns revealing finer structures than those discussed at the beginning of this section is

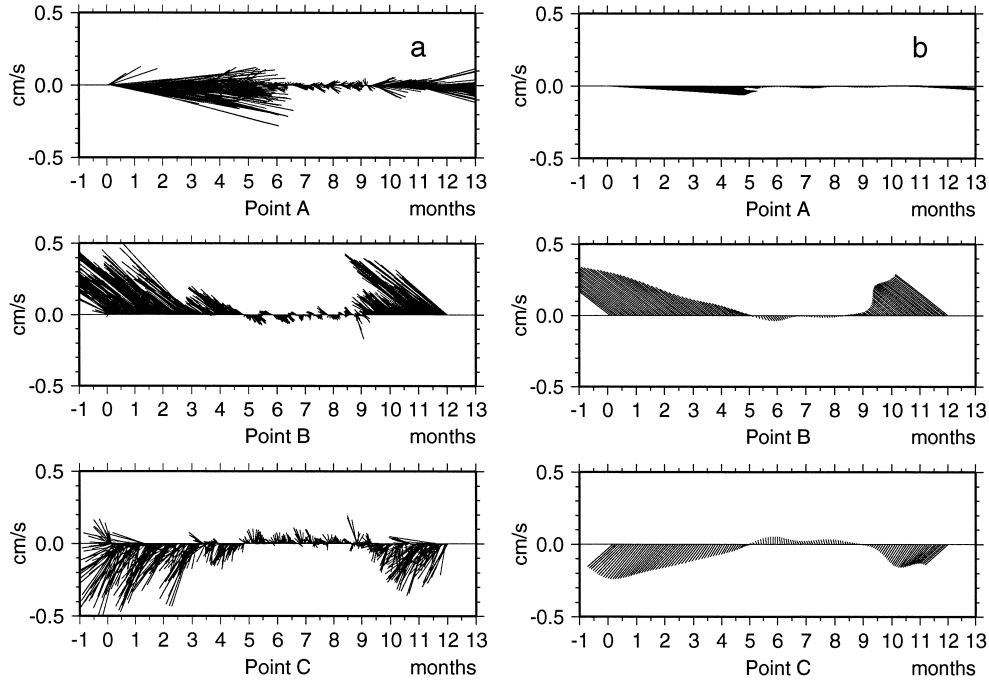

Fig. 5. (a) Stick-diagrams of the perpetual currents in points A, B and C of Fig. 1. (b) Currents Fourier filtered according to Eq. (3).

given in Figs. 6 and 7, where two snapshots of the filtered perpetual year transport $Q = H\eta$ on the 31st of January and 30th of June are shown, respectively.

As far as the winter is concerned (Fig. 6), apart form the basin-wide cyclonic circulation, well defined strait flows are present. In the strait of Sicily a strong horizontal shear in the wind-driven transport can be observed: the southward flow along the Tunisian coasts is accompanied by a northward flow that follows the western Sicilian shelf and eventually joins the internal cyclonic path. In the north waters separate from the internal gyre and flow northward through the strait of Corsica, after which they follow a cyclonic path in the Liguro–Provençal basin, which receives a further input from the northward flow west of Corsica. In the north of Tunisia, an anticyclonic flow is deflected by the local topography and, after having changed into a cyclonic motion is partly entrained by the internal cyclonic gyre and partly joins the southward Tunisian current. Note that the nearly barotropic cyclonic gyre east of the Strait of Bonifacio which is known to be fed almost year-round by the eastward wind jet from that strait (Moen, 1984; Artale et al., 1994; Perilli et al., 1995) is not reproduced by this model. This is due to the nature of the wind forcing used which does not resolve small scale wind features.

In summer (Fig. 7), an almost basin-wide, weak anticyclonic circulation is present (note the scale, different from that of Fig. 6). A southward flow along the eastern Corsica and Sardinia coasts appears to be induced by the southward flow through the strait of Corsica which, in turn, is sustained by the anticyclonic circulation in the eastern Ligurian sea. This gyre appears to be driven by the northward currents west of Corsica which, by flowing over the shallow depths north of the island receive a negative vorticity input. In this period of the year there is no positive wind vorticity input in the area sufficient to reverse the flow, so that an anticyclonic circulation is established (Astraldi and Manzella (1983), documented a clear weak reversal of the circulation in the eastern Ligurian sea in the period May–June 1979). The wind-induced currents in the straits of Sardinia and Sicily are very weak. The meandering jet that is visible in Fig. 6 flowing at the border of the south-

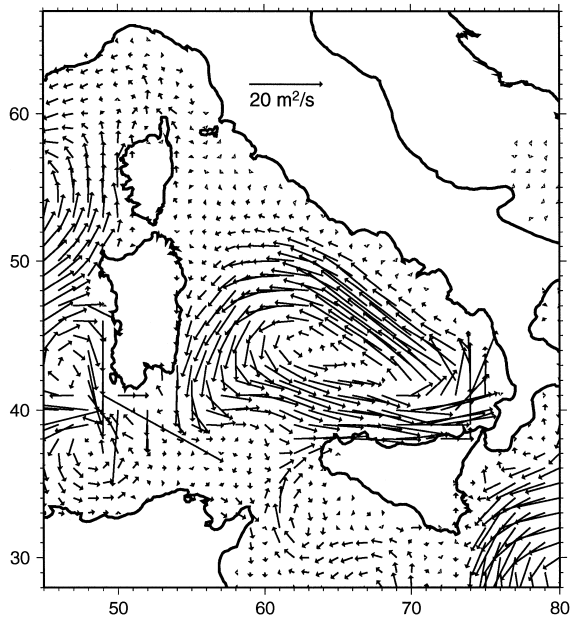

Fig. 6. Window of the Tyrrhenian Sea area: filtered perpetual transports on the 31st of January.

western Sicilian shelf and crossing the strait is now transformed into an anticyclonic gyre. The northward flow east of Tunisia appears to be blocked by the reversed circulation in the Tyrrhenian and, consequently overshoots to form a closed recirculation.

Among the smaller scale features evidenced in the last two figures, the flow regimes through the straits of Corsica and Sicily are the most relevant ones. It is well known that a strongly barotropic flow in the strait of Corsica is present year-round, and with a seasonal variability that reflects that found in this study (Astraldi and Gasparini, 1992, 1994; Astraldi et al., 1994). The problem of the extent to which the wind contributes to such transport will be addressed in Section 5, but we can already affirm that the nature of the local wind-driven circulation is the same as that observed in the strait of Corsica. On the contrary, in the strait of Sicily the situation is quite different. Here, a westward transport of LIW in the bottom layer is accompanied by an eastward transport of MAW, so to produce a vertically sheared current (e.g., Manzella et al., 1988; Manzella and La Violette, 1990; Moretti et al., 1993). A barotropic component of the current is however present, and only to that one can the present model results be compared with (note that high frequency barotropic circulation features in the strait are considered by Pierini (1996)). In this framework, it is interesting to notice the strong northward flow just off the Sicilian shelf which opposes to the southward flow along the Tunisian coasts. This indicates that the wind-driven barotropic component of the transport presents a strong horizontal shear across the strait, so that in evaluating the total barotropic transport through the strait one misses this feature, particularly important in winter months.

Finally, let us investigate the way the typical winter circulation evolves toward the typical summer circulation. From Fig. 5, it is evident that this transition takes place on average at the end of May. In Fig. 8, four snapshots of the filtered circulation from May 20 to June 20 are shown describing this process. On May 20, the situation is similar to that of Fig. 6, but with a reduced intensity and with the absence of the northward flow across the strait of Corsica. At the end of May, there is a further reduction of the circulation and a southward current from the north appears. On June 10, the latter contributes to the establishment of an anticyclonic gyre in the northern Tyrrhenian Sea, whose southern

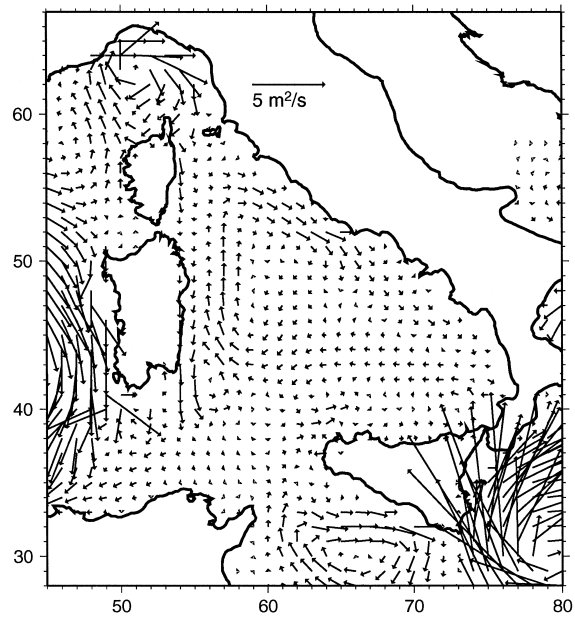

Fig. 7. Window of the Tyrrhenian Sea area: filtered perpetual transports on the 30th of June.

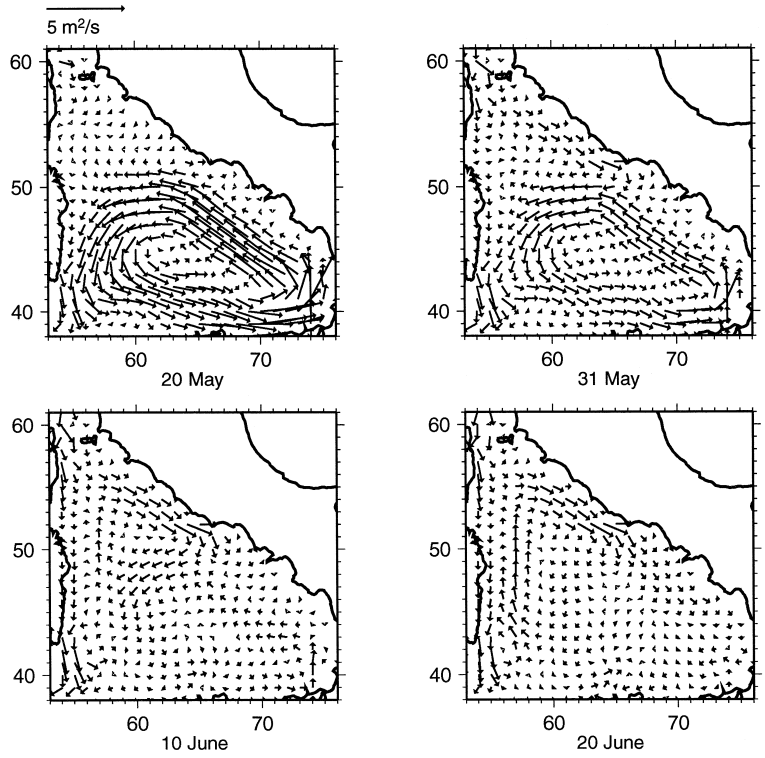

Fig. 8. Snapshots of filtered perpetual transports during the winter–summer transition.

branch joins the residual cyclonic circulation. Finally on June 20 we are in a typical summer scenario, where the northern anticyclonic gyre has now covered the whole basin, but with a stronger signal in the northeastern Tyrrhenian Sea.

The winter–summer transition in the Tyrrhenian Sea was associated in previous modelling studies (Pinardi and Navarra, 1993; Roussenov et al., 1995) to the appearance in the barotropic streamfunction of an anticyclonic gyre in the eastern part of the basin, subsequently shifting westward. The disagreement with the present results could be due to the different perpetual year forcing used (see Section 2), to the complete neglect in our model of the Jebar effect or/and to the absence of the thermal forcings. However, it is worth noticing that inquiring about the mode of transition between two distinct wind-driven circulation regimes in the climatological signal is little more than an academic exercise because, as we will see in Section 4, realistic instantaneous winds produce space and time variabilities that resemble transient perpetual features such as that just discussed only slightly or not at all.

4. The daily variability

The seasonal and longer term—interannual—variabilities (for which the typical time scale T is $T > O$ (1 month)) are the most distinctive features of each oceanic basin, because the character of the forcings and the geometry of the basin act together to produce a well defined seasonal climatology and its variation in the different years that is usually peculiar of the region of interest. This is why virtually all the modelling studies concerning the Mediterranean sea are focused on these particular aspects of the circulation, for which usually monthly averages of the momentum, heat, evaporative and lateral fluxes are considered.

At the other side of the spectrum ($T \leq O$ (1 day)), superinertial variabilities (such as gravity and inertia–gravity internal and surface waves, seiches, Kelvin waves, inertial currents, etc.) have not only very small time scales but also length scales usually much smaller than the basin under consideration, therefore, the basin geometry does not play a crucial role *as a whole* in determining their characteristics (the tides do depend in their shape and amplitude on the basin geometry but their variability is exactly determined, at least in principle). All these variabilities have clearly little to do with the Mediterranean circulation.

There is, however, an intermediate high frequency range (O(1 day) $< O$ (1 month)) for which the forcing mechanisms and the induced length scales are comparable to those typical of the seasonal variability, but whose response is filtered out when using the monthly mean forcings. Over these time scales, the changes of sensible and latent heat fluxes that induce mainly the thermohaline circulation, are not expected to determine an oceanic response comparable to the climatological one because of the slow baroclinic adjustment processes involved. For the winds, however, the situation is quite different: they vary over an 1-day time scale typical of the atmospheric weather systems and their r.m.s. is larger than the monthly mean, as shown for the Tyrrhenian Sea in Fig. 2. Moreover, the mechanism of generation of currents briefly described at the beginning of Section 2 allows for a fast barotropic adjustment. As a consequence, one could expect that over a period of few days a wind-driven signal is present in the Tyrrhenian Sea that can be comparable or even larger than the climatological one. The study of this kind of variability (here denoted as 'daily'), that the present free-surface model can describe correctly, is usually disregarded in modelling studies, but we believe its understanding is relevant for short-term ocean forecasting and for modelling properly the horizontal dispersion in the sea. At the best of the authors' knowledge the only study in which the high frequency wind-driven response in the Mediterranean was considered by Piacsek and Allard (1995).

We now pass to analyze the daily variability of the two test years 1981 and 1987. The year 1981 is particularly interesting because in the winter major episodes of anomalous wind amplitudes are present

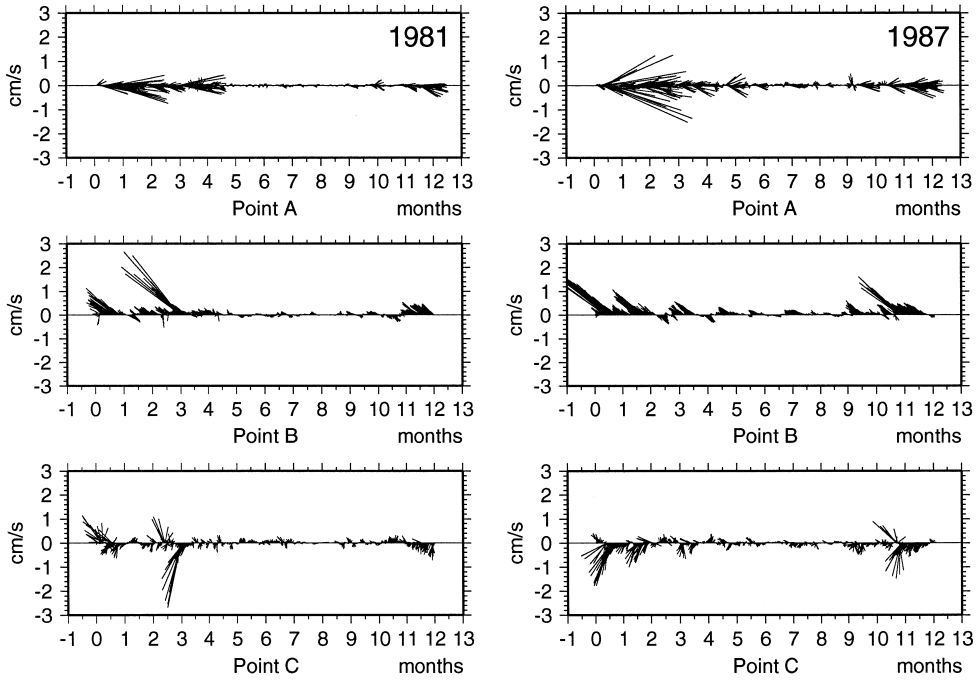

Fig. 9. Stick-diagrams of the instantaneous 1981 and 1987 currents in points A, B and C of Fig. 1.

(Pinardi et al., 1996); the year 1987 is chosen because current meter data are available in the strait of Corsica for that year (see Section 5 for a comparison between numerical and experimental data). We stress that the spin up in the present homogeneous model is very rapid (2–3 days), so that we performed single-year runs for the two test years.

In Fig. 9, the stick-diagrams referring to the points A, B and C of Fig. 1 are shown for the instantaneous 1981/1987 forcings. By comparing these currents with the *perpetual* ones (Fig. 5a) one can notice immediately two important differences. First of all, the instantaneous currents can be up to 10 times larger than the corresponding climatological ones, secondly, their variability is remarkably larger than the climatological one. For instance, in the perpetual year response, the currents in points B and C are coherently northwestward and southeastward, respectively, from the beginning of October until the end of May while in the instantaneous 1987 response they are predominantly in the same direction (though with a larger variance) but with periods of reversed circulation. In 1981 the situation is even more dramatically different: the variability until the end of April is such that one could hardly recognize the average winter condition. In both years the amplitude of the currents can sometime change by an order of magnitude in few days. The comparison of the stick-diagrams of Fig. 9a,b with the corresponding wind forcing in Fig. 2 allows to recognize easily the correlation between the positive (negative) spikes of wind stress curl and the corresponding cyclonic (anticyclonic) circulation induced in the Tyrrhenian Sea. See for instance the positive spike at the end of March 1981 and the corresponding intense cyclonic circulation induced, or the strong positive wind curl activity in mid-January and mid-February 1987 and the positive vorticity driven inside the basin.

In order to obtain a synoptic view of the current patterns associated to typical transient events and nearly steady conditions a series of snapshots referring to 6 consecutive days are given in Figs. 10–13. Fig. 10 shows the situation during the third week of March 1981 when, as can be seen in Fig. 9a, the daily variability was relevant. In the six pictures, a cyclonic gyre is always detectable but its shape and location varies remarkably; at the same time a complete reversal and counter-reversal of the current can

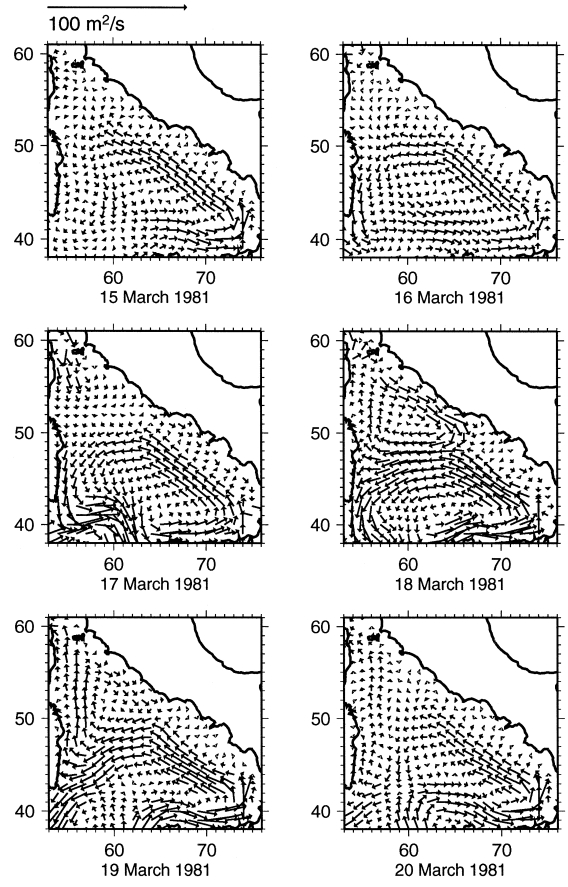

Fig. 10. Snapshots of instantaneous transports.

be observed along Sardinia and Corsica (15/17/19 March) and the generation and disappearance of two anticyclonic gyres along the Italian coasts and their movement is also evident. In Fig. 11 a period of analogous strong daily variability is shown referring to the 3rd week of November 1987. A relatively weak cyclonic circulation located in the southern part of the basin evolves toward a much stronger one embracing the whole Tyrrhenian Sea; at intermediate times an anticyclonic gyre formed on November 20 in the north moves southward along the Sardinian coast and eventually looses its individuality at the end of the week. Finally, in Figs. 12 and 13 two more stable situations are presented. In Fig. 12 the week initiated with the large positive wind stress spike in late March 1981 mentioned above is reported. The intense basin-wide cyclonic circulation

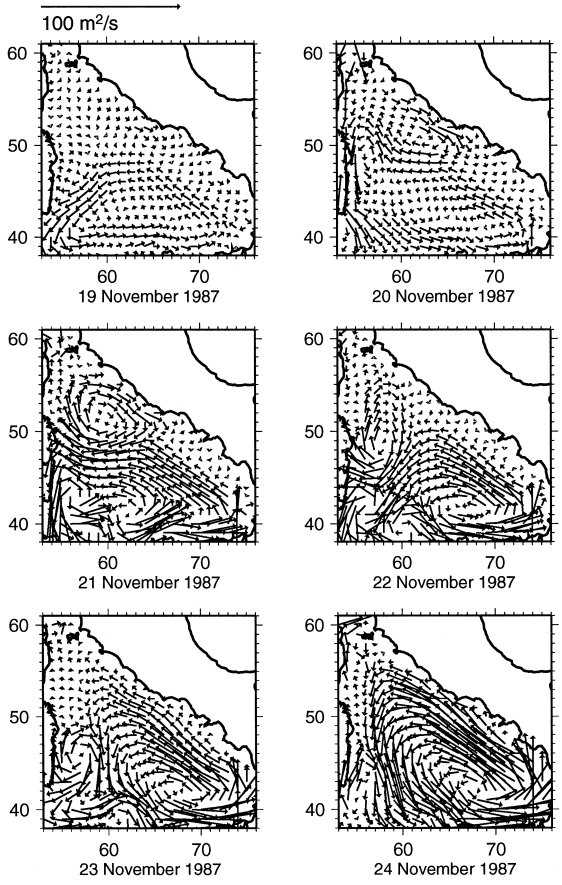

Fig. 11. Snapshots of instantaneous transports.

undergoes oscillations but always retains its structure; only some meandering currents in the north can be observed. Fig. 13 corresponds to a cyclonic circulation during a period of decreasing trend in the second half of January 1987 (see Fig. 9b). Here, the spatial structure of the gyre varies very little but the weakening of the currents is evident.

As far as the experimental evidence of the presence of this high frequency variability is concerned, no current time series (the only data relevant for this purpose) in the deep sea are available, but data of this kind were obtained in the shallow waters of the northern Tyrrhenian Sea and off Corsica. Elliott (1979) and Astraldi and Manzella (1983) reported barotropic currents off the northwest Italian coasts and on the East Ligurian shelf, respectively, having a large high frequency variability clearly induced by the winds. Astraldi et al. (1990) presented current time series west of Corsica and in the strait, both yielding large fluctuations over a 2 day/1 week time scale (note that the data were low-pass filtered to remove oscillations below 2 days). Artale et al. (1994) showed current data gathered in the northern Tyrrhenian Sea. No direct comparison with the present numerical results is possible because those data refer to the years 1989–1990 that are not included in the wind data set used, and also because they are taken in a region in which a gyre not resolved by our winds is present (see Section 3). However, the stick-diagrams reveal a pronounced high frequency variability that is much more like that shown in Fig. 9 rather than that of Fig. 5a, with several episodes of reversal of the currents not to be expected in the seasonal signal. All these current data confirm quali-

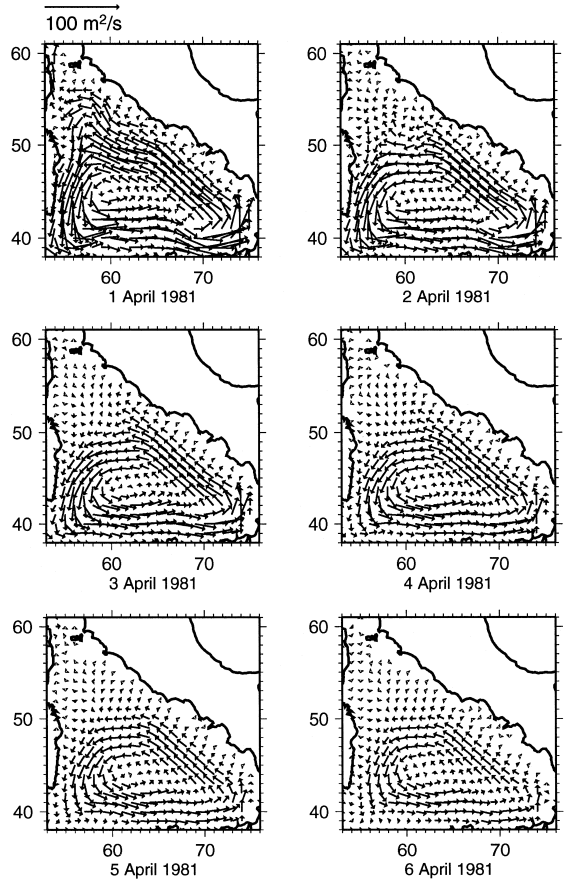

Fig. 12. Snapshots of instantaneous transports.

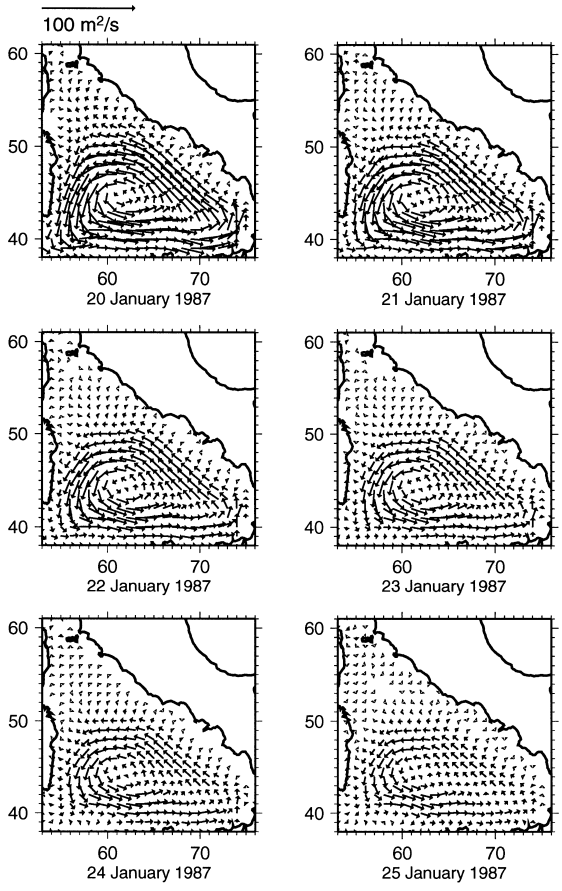

Fig. 13. Snapshots of instantaneous transports.

tatively the existence of a remarkable high frequency variability of the currents in the Tyrrhenian Sea area.

One last point that we want to address is the dynamical character of the wind-driven daily variability. In Section 2 we recounted the well known mechanisms through which Ekman and geostrophic currents are induced by the wind. The consequent direct response to winds, shaped by the geometrical characteristics of the basin, determine to a large extent the oceanic response. However, also internal dynamical mechanisms can contribute to determine the form of the barotropic response. Apart from cases of barotropic instability, this is typically due to the existence of wave systems that are excited by the wind but whose temporal and spatial features are not necessarily directly reminiscent of the wind forcing. Here, we do not refer to long gravity waves (which are, however, included in the shallow-water dynamics), whose frequencies are well beyond the temporal range of interest, but rather to rotational waves such as continental shelf and topographic and planetary Rossby waves and modes. Elliott (1979) considered the existence of continental shelf waves along the coast of northwest Italy, although no definitive evidence of their existence could be provided, the possibility remains that such a coastal wave activity in the area with periods of about 5 days may be present. Pierini (1996) showed that resonant topographic Rossby modes could be excited by the wind and remote currents in the strait of Sicily with periods ranging from 2 to 5 days. The Tyrrhenian Sea has coastal and topographical characteristics that could —in principle—allow for the existence of similar waves or modes. On the other hand, the overwhelming action of the topographic steering appears to prevent the existence of the planetary dynamics in the Tyrrhenian Sea (Pierini, 1997). In conclusion, further studies in this direction are needed in order to get a deeper understanding of the intrinsic dynamical features of the wind-driven circulation of the basin.

5. Discussion and conclusions

In Sections 3 and 4 the seasonal and high frequency wind-driven currents in the Tyrrhenian Sea area have been analyzed in the framework of a numerical process study, and a significant qualitative agreement with previous experimental and theoretical studies has been found. At this stage, an important point that should be analyzed is the relative weight of the wind-driven circulation in comparison with motions of different origin, because understanding how the energy and transports are partitioned into the various dynamical components is the basis for a satisfactory description of the circulation of a basin. A comparison of the present numerical results with experimental observations and theories will provide some quantitative indications to this respect.

Let us thus focus on the dynamics of the strait of Corsica, which is a good indicator of the global Tyrrhenian circulation and for which valuable current meter measurements are available. This is a very narrow channel, its width being approximately equal

to the spatial resolution of the present model (25 km). Numerical currents taken at a specific grid point cannot, therefore, be compared with experimental currents taken in the strait, but the total transport across it can, instead, be used in relation with data. Fig. 14a shows the transport across line L1 (see Fig. 1) for the year 1987 described in Section 4. A predominant northward flux is found in the periods January–April and October–December while a predominant but weaker southward flux can be observed in the rest of the year; remarkable is the daily variability, as expected from the discussion of Section 4. The transport has episodes of up to 1.3 Sv in January, 0.8–1 Sv in other winter and autumn months and ± 0.2–0.4 Sv in summer. The 50-day running mean filtered transport (computed on the signal assumed periodic) has a maximum value of 0.25 Sv at the end of January and a minimum value of about -0.05 Sv in summer. Astraldi et al. (1990) presented a 50-day running mean filtered transport of the local AW and LIW through the strait from October 1986 to September 1987. Only the seasonal trend was therefore left and the values ranged from a maximum of 1.4 Sv at the end of January 1987 (like for our filtered transport) to about 0.2 Sv in August for the total MAW-LIW transport.

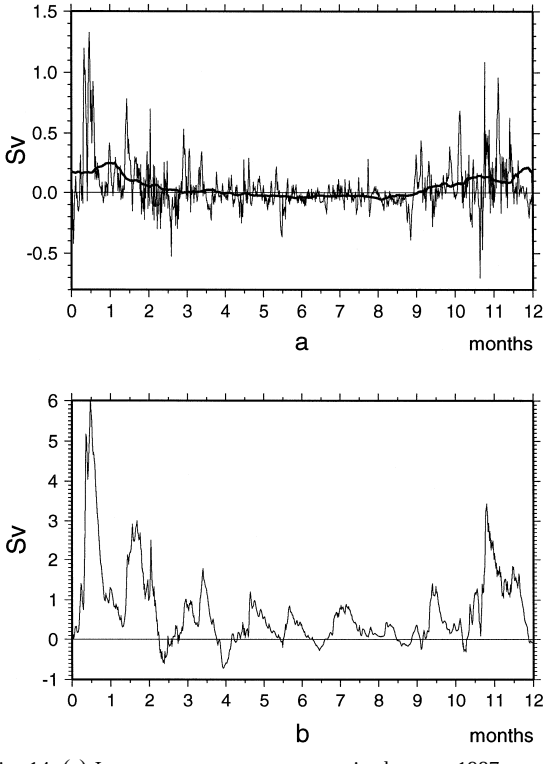

Fig. 14. (a) Instantaneous mass transport in the year 1987 across line L1 of Fig. 1 and 50-day running mean filtered transport. (b) Instantaneous mass transport in the year 1987 across line L2 of Fig. 1.

Hence, our numerical seasonal wind-driven transport in 1987 appears to be only a fraction, 15–20% of the total transport, but the numerical high frequency variability shows fluctuations that can be as high as the experimental mean seasonal signal. These large fluctuations are not shown in the filtered transport of Astraldi et al. (1990), but currents in the strait low-pass filtered only below 2 days, presented in the same paper, do reveal variations of the same frequency and amplitude as the present numerical results.

It should be stressed that the above numerical transport estimate is obtained for $A_H = 5000$ m^2/s, which is about 10 times larger than typical values used in models with an $1/4°$ resolution. This anomalously high value was required in the high frequency runs, in which the large temporal and spatial gradients of the wind forcing would, otherwise, produce numerical instabilities; the same choice was then made also in the seasonal runs, for the sake of consistency. However, short term integrations with lower values of A_H carried out until the onset of instabilities show responses similar to those presented in this paper, but with larger amplitudes. For example, the choice $A_H = 500$ m^2/s would produce amplitudes about twice as large as those shown here. Therefore the above transport estimate could be corrected to 15–40% for a range of values 5000 to 500 m^2/s for the horizontal eddy viscosity coefficient.

In conclusion, one can envisage the following scenario for the strait of Corsica transport in the year 1987.

(a) A constantly northward *seasonal* transport is present, with values ranging from 1.4 Sv in winter to 0.2 Sv in summer (Astraldi et al., 1990). According to the present model, the wind-driven seasonal transport may have accounted for 15–40% of the total.

(b) A significant *high frequency* variability modulates the seasonal transport. It is mainly induced by the wind and its r.m.s. is comparable to the seasonal signal. The present model results show a total wind-

driven flux with peaks as high as 0.8–1.3 Sv in winter and ± 0.2–0.4 Sv in summer for $A_H = 5000$ m^2/s (values are about twice as large for $A_H = 500$ m^2/s).

A question now arises: what is the cause of the nonwind-driven part of the seasonal transport in the strait of Corsica? The main contribution is believed to be due to gradients of heat losses in winter between the Tyrrhenian Sea and the Liguro–Provençal basin, and to the remote mass flux through the strait of Gibraltar. The amount of sensible and latent heat lost in winter in the Liguro–Provençal basin because of air–sea interactions and of deep water formation processes in the Gulf of Lions is larger than that lost in the Tyrrhenian Sea, so that a steric level gradient between the two basins is produced which forces a northward mass flux through the strait of Corsica (Astraldi and Gasparini, 1992). On the other hand, the opposite fluxes of AW and LIW through the strait of Gibraltar are shown to be able to account for 0.32–0.7 Sv in the strait of Corsica transport (Herbaut et al., 1996). The nature of these two effects is such that their contribution to the strait flux is mainly concentrated at low frequencies (the seasonal variability), while it is the wind that induces the rapid, intense current activity.

Finally, we pass to analyze the interaction between the wind-driven dynamics in the straits of Corsica, Sicily and Sardinia and that in the interior of the Tyrrhenian Sea. By clarifying this point, one would get some information on how to infer dynamical characteristics of the Tyrrhenian Sea by studying the fluxes through the straits (the preceding discussion is an example) where measurements can more easily be carried out. In Fig. 14b, the transport across line L2 (see Fig. 1) for the year 1987 is reported, showing the intensity and variability of the main Tyrrhenian gyre at its eastern branch. The signal is qualitatively similar to that of the strait of Corsica shown in Fig. 14a, but its amplitude is about 5 times larger, reaching a maximum value of 6 Sv in January. This suggests that there is probably a one-way interaction: the Tyrrhenian wind-driven dynamics is basically due to the local winds, and the flux through the strait of Corsica depends mainly on the regime of circulation at its southern boundary. Inversely, the

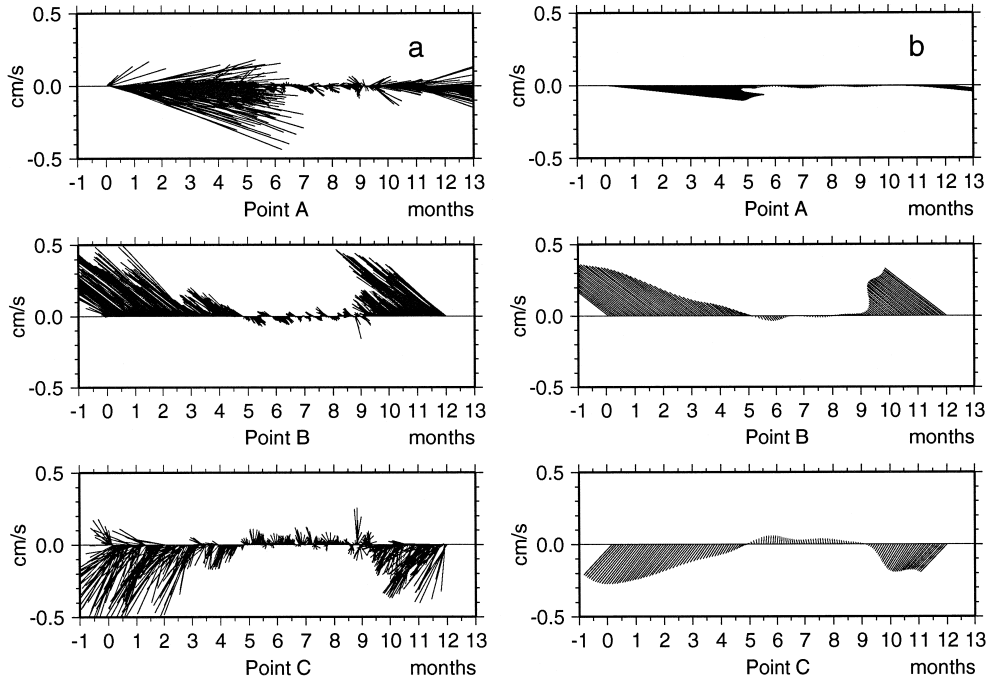

Fig. 15. (a) Stick-diagrams of the perpetual currents in points A, B and C of Fig. 1 for the closed Tyrrhenian Sea case. (b) Currents Fourier filtered according to Eq. (3) for the closed Tyrrhenian Sea case.

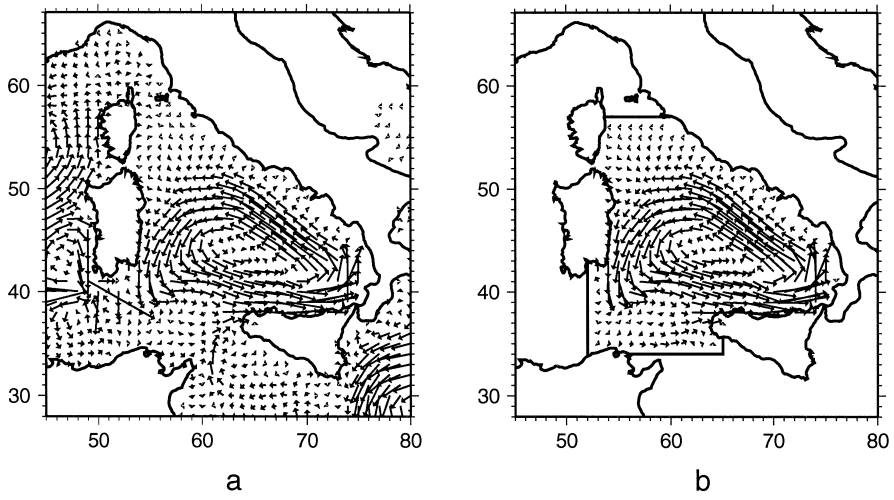

Fig. 16. Filtered perpetual transports on the 31st of January for the open (a) and closed (b) Tyrrhenian Sea case.

flux through the strait can hardly contribute to determine the internal Tyrrhenian circulation, being so much weaker than the latter.

This hypothesis is confirmed, also for the straits of Sicily and Sardinia, in the following sensitivity experiment. The seasonal variability is studied in a 'closed' Tyrrhenian Sea (see Fig. 16b) and is then compared with that obtained in the framework of the whole Mediterranean. Fig. 15 shows the perpetual instantaneous and filtered currents in points A, B and C for the closed sea case. A comparison with Fig. 5 immediately puts in evidence the almost identical response between the open and closed sea cases. Figs. 16 and 17 show the comparison between the two responses on January 31 and June 30, respectively. The flows are virtually identical in the interior while they obviously differ near the straits. The only significant difference in the interior is found in sum-

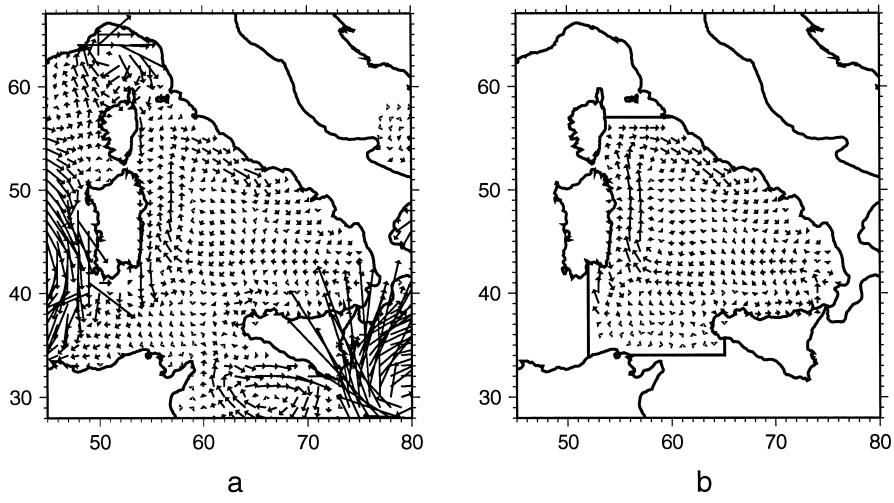

Fig. 17. Filtered perpetual transports on the 30th of June for the open (a) and closed (b) Tyrrhenian Sea case.

mer along the western Corsica and Sardinia coasts: the southward coastal current is greatly reduced in amplitude in the closed sea case, in agreement with its explanation given in Section 3. This is a Tyrrhenian wind-driven feature that is mainly forced by the anticyclonic gyre induced in summer in the Ligurian sea, so neglecting this effect virtually eliminates this current. Therefore, apart from this specific coastal current, one can conclude that the wind-driven dynamics in the Tyrrhenian Sea is basically induced by the local winds on a basin scale and is largely independent on the wind-driven response in the rest of the Mediterranean. On the other hand, the wind-driven currents through the Corsica, Sicily and Sardinia straits are forced by the Tyrrhenian Sea dynamics, but they also depend on local and remote wind effects. It goes without saying that these conclusions apply strictly to the wind-driven dynamics. The water mass characteristics of the Tyrrhenian Sea in terms of LIW and MAW are heavily dependent on the flows through the straits of Sicily and Sardinia, which provide a pathway for the intrusion of those waters from the eastern and western Mediterranean subbasins.

Acknowledgements

This research was funded by the European Union contract MAS2-CT93-0055 'MERMAIDS II'. We would like to thank N. Pinardi, M. Astraldi and G.P. Gasparini for helpful discussions. N. Pinardi also provided the 'National Meteorological Center' wind data, the use of which is kindly acknowledged.

References

Artale, V., Astraldi, M., Buffoni, G., Gasparini, G.P., 1994. Seasonal variability of gyre-scale circulation in the northern Tyrrhenian Sea. J. Geophys. Res. 99, 14127–14137.

Astraldi, M., Gasparini, G.P., 1992. The seasonal characteristics of the circulation in the North Mediterranean basin and their relationship with the atmospheric-climatic conditions. J. Geophys. Res. 97, 9531–9540.

Astraldi, M., Gasparini, G.P., 1994. The seasonal characteristics of the circulation in the Tyrrhenian Sea. In: La Violette, P. (Ed.), Seasonal and Interannual Variability of the Western Mediterranean Sea. Coastal and Estuarine Studies, Vol. 46. American Geophysical Union, pp. 115–134.

Astraldi, M., Manzella, G.M.R., 1983. Some observations on current measurements on the east Ligurian shelf, Mediterranean Sea. Continental Shelf Res. 2, 183–193.

Astraldi, M., Gasparini, G.P., Manzella, G.M.R., Hopkins, T.S., 1990. Temporal variability of currents in the eastern Ligurian Sea. J. Geophys. Res. 95, 1515–1522.

Astraldi, M., Gasparini, G.P., Sparnocchia, S., 1994. The seasonal and interannual variability in the Ligurian–Provençal basin. In: La Violette, P. (Ed.), Seasonal and Interannual Variability of the Western Mediterranean Sea. Coastal and Estuarine Studies, Vol. 46. American Geophysical Union, pp. 93–113.

Beckers, J.M., 1991. Application of a 3D model to the Western Mediterranean. J. Mar. Syst. 1, 315–332.

Beckers, J.M., Brasseur, P., Djenidi, S., Nihoul, J.C.J., 1994. Investigation of the Western Mediterranean's hydrodynamics with the Gher three-dimensional primitive equation model. In: La Violette, P. (Ed.), Seasonal and Interannual Variability of the Western Mediterranean Sea. Coastal and Estuarine Studies, Vol. 46. American Geophysical Union, pp. 287–324.

Béthoux, J.P., 1980. Mean water fluxes across sections in the Mediterranean Sea evaluated on the basis of water and salt budgets and of observed salinities. Oceanol. Acta 3, 79–88.

Elliott, A.J., 1979. Low-frequency sea level and current fluctuations along the coast of northwest Italy. J. Geophys. Res. 84, 3752–3760.

Heburn, G.W., 1987. The dynamics of the Western Mediterranean Sea: a wind forced case study. Ann. Geophys. 5B, 61–74.

Heburn, G.W., 1994. The dynamics of the seasonal variability of the Western Mediterranean circulation. In: La Violette, P. (Ed.), Seasonal and Interannual Variability of the Western Mediterranean Sea. Coastal and Estuarine Studies, Vol. 46. American Geophysical Union, pp. 249–285.

Herbaut, C., Mortier, L., Crépon, M., 1996. A sensitivity study of the general circulation of the Western Mediterranean Sea: I. The response to density forcing through the straits. J. Phys. Oceanogr. 26, 65–84.

Herbaut, C., Martel, F., Crépon, M., 1997. A sensitivity study of the general circulation of the Western Mediterranean Sea: II. Response to atmospheric forcing. J. Phys. Oceanogr. 27, 2126–2145.

Holland, W.R., 1973. Baroclinic and topographic influences on the transport in western boundary currents. Geophys. Fluid Dyn. 4, 187–210.

Hopkins, T.S., 1988. Recent observations on the intermediate and deep water circulation in the southern Tyrrhenian Sea. Oceanol. Acta 9, 41–50.

Huthnance, J.M., 1984. Slope currents and 'JEBAR'. J. Phys. Oceanogr. 14, 795–810.

Korres, G., Pinardi, N., Lascaratos, A., 1995a. The seasonal and interannual variability of the Mediterranean Sea: I. Model simulations. Submitted.

Korres, G., Pinardi, N., Lascaratos, A., 1995b. The seasonal and interannual variability of the Mediterranean Sea: II. Empirical orthogonal functions analysis. Submitted.

Krivosheya, V.G., Ovchinnikov, I.M., 1973. Properties of the geostrophic circulation of the Tyrrhenian Sea. Oceanology 13, 996–1002.

Malanotte-Rizzoli, P., Bergamasco, A., 1989. The circulation of the eastern Mediterranean: I. Oceanol. Acta 12, 335–351.

Malanotte-Rizzoli, P., Bergamasco, A., 1991. The wind and thermally driven circulation of the eastern Mediterranean Sea: II. The baroclinic case. Dyn. Atmos. Oceans 15, 355–371.

Manzella, G.M.R., La Violette, P.E., 1990. The seasonal variation of water mass content in the western Mediterranean and its relationship with the inflows through the straits of Gibraltar and Sicily. J. Geophys. Res. 95, 1623–1626.

Manzella, G.M.R., Gasparini, G.P., Astraldi, M., 1988. Water exchange between the eastern and western Mediterranean through the strait of Sicily. Deep-Sea Res. 35, 1021–1035.

Millot, C., 1987. Circulation in the western Mediterranean Sea. Oceanol. Acta 10, 143–149.

Moen, J., 1984. Variability and mixing of the surface layer in the Tyrrhenian Sea: MILEX-80, final report. SACLANTCEN Rep. SR-75, SACLANTCEN Research Center, La Spezia, Italy, 128 pp.

Moretti, M., Sansone, E., Spezie, G., De Maio, A., 1993. Results of investigations in the Sicily Channel (1986–1990). Deep-Sea Res. 40, 1181–1192.

Pedlosky, J., 1987. Geophysical Fluid Dynamics. Springer-Verlag, New York.

Perilli, A., Rupolo, V., Salusti, E., 1995. Satellite investigations of a cyclonic gyre in the central Tyrrhenian Sea (western Mediterranean Sea). J. Geophys. Res. 100, 2487–2499.

Piacsek, S., Allard, R., 1995. Barotropic coastal currents in the Mediterranean. Global Ocean Atmos., submitted.

Pierini, S., 1996. Topographic Rossby modes in the strait of Sicily. J. Geophys. Res. 101, 6429–6440.

Pierini, S., 1997. Westward intensified and topographically modified planetary modes. J. Phys. Oceanogr. 27, 1459–1471.

Pierini, S., Zambianchi, E., 1997. Chaotic advection and turbulent diffusion in Rossby waves in a closed basin. Submitted.

Pierrehumbert, R.T., 1990. Chaotic mixing of tracer and vorticity by modulated travelling Rossby waves. Geophys. Astrophys. Fluid Dyn. 58, 285–319.

Pinardi, N., Korres, G., Lascaratos, A., Roussenov, V., Stanev, E., 1996. Numerical simulation of the interannual variability of the Mediterranean Sea upper ocean circulation. Geophys. Res. Lett., in press.

Pinardi, N., Navarra, A., 1993. Baroclinic wind adjustment processes in the Mediterranean Sea. Deep-Sea Res. 40, 1299–1326.

Robinson, A.R., Colnaraghi, M., Leslie, W.G., Artegiani, A., Hecht, A., Lazzoni, E., Michelato, A., Sansone, E., Theocharis, A., Unlüata, U., 1991. Structure and variability of the eastern Mediterranean general circulation. Dyn. Atmos. Oceans 15, 215–240.

Roussenov, V., Stanev, E., Artale, V., Pinardi, N., 1995. A seasonal model of the Mediterranean Sea general circulation. J. Geophys. Res. 100, 13515–13538.

Smith, S.D., 1980. Wind stress and heat flux over the ocean in gale force winds. J. Phys. Oceanogr. 10, 709–726.

Stanev, E.V., Friedrich, H.J., Botev, S., 1989. On the seasonal response of intermediate and deep water to surface forcing in the Mediterranean sea. Oceanol. Acta 12, 141–149.

Tziperman, E., Malanotte-Rizzoli, P., 1991. The climatological seasonal circulation of the Mediterranean Sea. J. Mar. Res. 49, 411–434.

Zavatarelli, M., Mellor, G.L., 1995. A numerical study of the Mediterranean Sea circulation. J. Phys. Oceanogr. 25, 1384–1414.